Structural Engineering and Mechanics, *Vol. 51, No. 6 (2014) 939-953*
DOI: http://dx.doi.org/10.12989/sem.2014.51.6.939

Displacements and stresses in pressurized thick FGM cylinders with exponentially varying properties based on FSDT

Mehdi Ghannad[a] and Hamed Gharooni[*]

Department of Mechanical Engineering, Shahrood University of Technology, Shahrood, Iran

(Received April 24, 2012, Revised May 4, 2014, Accepted May 18, 2014)

Abstract. Using the infinitesimal theory of elasticity and analytical formulation based on the first-order shear deformation theory (FSDT) is presented for axisymmetric thick-walled cylinders made of functionally graded materials under internal and/or external uniform pressure. The material is assumed to be isotropic heterogeneous with constant Poisson's ratio and radially exponentially varying elastic modulus. At first, general governing equations of the FGM thick cylinders are derived by assumptions of the FSDT. Then the obtained equations are solved under the generalized clamped-clamped conditions. The results are compared with the findings of both FSDT and finite element method (FEM).

Keywords: thick cylinders; shear deformation theory; exponential; FGM; FSDT; FEM

1. Introduction

Axisymmetric hollow cylinders are important in industries. In order to optimize the weight, mechanical strength, displacement and stress distribution of a shell, one approach is to use shells with functionally graded materials (FGMs). FGMs or heterogeneous materials are advanced composite materials with microscopically inhomogeneous characters. The first order displacement field (FSDT) for homogeneous thick cylindrical shells was expressed by Mirsky and Hermann (1958). Greenspon (1959) compared the results of different theories of thick-walled cylindrical shells. Fukui and Yamanaka (1992) used the Navier solution for derivation of the governing equation of a thick-walled FGM tube under internal pressure and solved the obtained equation numerically by means of the Runge-Kutta method. Simkins (1994) used the FSDT for determining displacement in a long and thick tube subjected to moving loads. Eipakchi *et al.* (2003) have investigated the governing equations of homogeneous cylinders with variable thickness using FSDT and represent the solution of the equations using perturbation theory. They further (2008) extended their previous work by considering homogenous and isotropic conical shells with variable thickness using FSDT and SSDT (second-order shear deformation theory) and solve the conducted equations by perturbation theory.

Hongjun *et al.* (2006) indicated the exact solution of FGM hollow cylinders in the state of plane strain with exponential function of elasticity modulus along the radius. Zhifei *et al.* (2007)

∗Corresponding author, Ph.D. Student, E-mail: Gharooni.hamed@gmail.com
[a]Assistant Professor, E-mail: Ghannad.mehdi@gmail.com

http://www.techno-press.org/?journal=sem&subpage=8 ISSN: 1225-4568 (Print), 1598-6217 (Online)

analyzed heterogeneous cylindrical shells with power function of elasticity modulus by the usage of multilayer method with homogeneous layers. Thick-walled FGM cylinders in plane strain state with exponentially-varying material properties were solved by Tutuncu (2007) using Frobenius method. Zamani Nejad *et al.* (2009) developed 3D set of field equations of FGM thick shells of revolution in curvilinear coordinate system by tensor calculus. Ghannad *et al.* (2010) present the general method of derivation and the analysis of an internally pressurized thick-walled cylinders with clamped-clamped ends. They (2012) presented a complete elastic solution of pressurized thick cylindrical shells made of heterogeneous functionally graded materials by the usage of plane elasticity theory.

Taking into account the effect of shear stresses and strains, the general method of derivation and the analysis of an internally and/or externally pressurized thick-walled cylindrical shells made of functionally graded material with constant Poisson's ratio and radially exponentially varying elastic modulus. The obtained equations are solved under the generalized clamped-clamped conditions. The results are compared with the findings of both FSDT and FEM.

2. Problem formulation

In shear deformation theory (SDT), the straight lines perpendicular to the central axis of the cylinder do not necessarily remain unchanged after loading and deformation, suggesting that the deformations are axial axisymmetric and change along the longitudinal cylinder. In other words, the elements have rotation, and the shear strain is not zero. The displacement field is assumed as a polynomial of a variable (z) through the thickness. As the number of terms in the polynomial function increase, the approximate solution will be improved. The first-order shear deformation theory (FSDT) is employed to simulate the deformation of every layer of the cylinder (Mirsky and Hermann 1958).

Where the parameter r, is the radius of every layer of cylinder which can be replaced in terms of radius of mid-plane R and distance of every layer with respect to mid-plane z as follows (Fig. 1)

$$r = R + z \tag{1}$$

x and z are the length and the thickness variables. The parameters x and z have been changed in the following intervals

$$0 \le x \le L \ \ , \ -\frac{h}{2} \le z \le +\frac{h}{2} \tag{2}$$

Where h and L are the thickness and the length of the cylinder.

Based on FSDT, every component of deformation can be stated by two variables that includes the displacement and rotation. For an axisymmetric cylindrical shell, axial and radial components of displacement field may be regarded as follows (Ghannad *et al.* 2010).

$$\begin{Bmatrix} U_x \\ U_\theta \\ U_z \end{Bmatrix} = \begin{Bmatrix} u(x) \\ 0 \\ w(x) \end{Bmatrix} + \begin{Bmatrix} \varphi(x) \\ 0 \\ \psi(x) \end{Bmatrix} z \tag{3}$$

Where $u(x)$ and $w(x)$ are the displacement components of the middle surface. Also, $\phi(x)$ and $\psi(x)$ are the functions used to determine the displacement field.

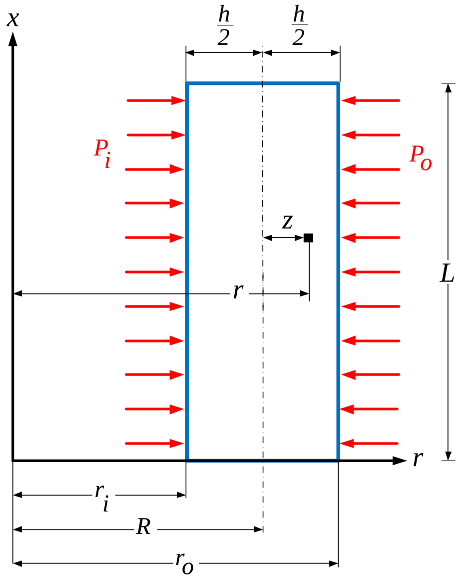

Fig. 1 Geometry of the thick pressurized cylindrical shell

The mechanical kinematic relations in the cylindrical coordinates system for an axisymmetric cylinder are

$$\begin{cases} \begin{Bmatrix} \varepsilon_x \\ \varepsilon_\theta \\ \varepsilon_z \end{Bmatrix} = \begin{Bmatrix} \dfrac{\partial U_x}{\partial x} \\ \dfrac{U_z}{r} \\ \dfrac{\partial U_z}{\partial z} \end{Bmatrix} = \begin{Bmatrix} \dfrac{du}{dx} \\ \dfrac{w}{R+z} \\ \psi \end{Bmatrix} + \begin{Bmatrix} \dfrac{d\varphi}{dx} \\ \dfrac{\psi}{R+z} \\ 0 \end{Bmatrix} z \\ \gamma_{xz} = \dfrac{\partial U_x}{\partial z} + \dfrac{\partial U_z}{\partial x} = \left(\varphi + \dfrac{dw}{dx} \right) + \dfrac{d\psi}{dx} z \end{cases} \tag{4}$$

Modulus of elasticity E is assumed to be radially exponentially dependent and is assumed to vary as follows

$$E(r) = E_i e^{n\left(\frac{r}{r_i}-1\right)} = E_i e^{n\left(\frac{R+z}{r_i}-1\right)} \tag{5}$$

Here E_i is the modulus of elasticity at the inner surface r_i and n is the inhomogeneity constant determined empirically. Since the analysis was done for a thick wall cylindrical pressure vessel of isotropic FGM, and given that the variation of Poisson's ratio (ν) for engineering materials is small, the Poisson's ratio is assumed as constant.

The range $-1 \le n \le +1$ to be used in the present study covers all the values of coordinate exponent encountered in the references cited earlier. However, these values for n do not necessarily represent a certain material.

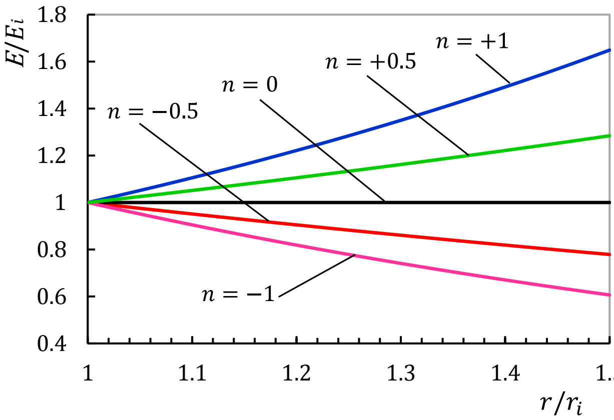

Fig. 2 Distribution of normalized elasticity modulus in FGM cylinder

Fig. 2 shows the distribution of normalized elasticity modulus with respect to the normalized radius in a heterogeneous cylinder for integer values of n.

On the basis of the constitutive equations for inhomogeneous and isotropic materials, the stress-strain relations are as follows

$$\begin{cases} \begin{Bmatrix} \sigma_x \\ \sigma_\theta \\ \sigma_z \end{Bmatrix} = \lambda E(z) \begin{bmatrix} 1-\nu & \nu & \nu \\ \nu & 1-\nu & \nu \\ \nu & \nu & 1-\nu \end{bmatrix} \begin{Bmatrix} \varepsilon_x \\ \varepsilon_\theta \\ \varepsilon_z \end{Bmatrix} \\ \tau_{xz} = \lambda E(z) \left[(1-2\nu) \dfrac{\gamma_{xz}}{2} \right] \end{cases} \tag{6}$$

Where the parameter λ is the constant value as follows

$$\lambda = \frac{1}{(1+\nu)(1-2\nu)} \tag{7}$$

Distribution of elasticity modulus basis on Eq. (1) and Eq. (5) is

$$E(z) = E_i e^{\left(\frac{nh}{2r_i}\right)} e^{\frac{nz}{r_i}} = \overset{*}{E}_i e^{n\left(\frac{z}{r_i}\right)} \tag{8}$$

The normal forces (N_x, N_θ, N_z), shear force (Q_x), bending moments (M_x, M_θ, M_z), and the torsional moment (M_{xz}) in terms of stress resultants are

$$\{N_x, N_\theta, N_z\} = \int_{-h/2}^{+h/2} \left\{ \sigma_x \left(1+\frac{z}{R}\right), \sigma_\theta, \sigma_z \left(1+\frac{z}{R}\right) \right\} dz \tag{9}$$

$$\{M_x, M_\theta, M_z\} = \int_{-h/2}^{+h/2} \left\{ \sigma_x \left(1+\frac{z}{R}\right), \sigma_\theta, \sigma_z \left(1+\frac{z}{R}\right) \right\} z dz \tag{10}$$

$$Q_x = K \int_{-h/2}^{+h/2} \tau_{xz} \left(1+\frac{z}{R}\right) dz \tag{11}$$

$$M_{xz} = K \int_{-h/2}^{+h/2} \tau_{xz} \left(1+\frac{z}{R}\right) z dz \tag{12}$$

K is the shear correction factor that is embedded in the shear stress term. It is assumed, in the static state, for conical shells K=5/6.

In order to drive the differential equations of equilibrium, the principle of virtual work have been used as

$$\delta U = \delta W \tag{13}$$

Where U is the total strain energy of the elastic body and W is the total external work due to internal and/or external pressure. The strain energy is

$$\begin{cases} U = \iiint_V U^* dV \quad , \; dV = r dr d\theta dx = \left(R + z\right) dx d\theta dz \\ U^* = \frac{1}{2}\{\varepsilon\}^T \{\sigma\} = \frac{1}{2}\left(\sigma_x \varepsilon_x + \sigma_\theta \varepsilon_\theta + \sigma_z \varepsilon_z + \tau_{xz}\gamma_{xz}\right) \end{cases} \tag{14}$$

and the external work is

$$\begin{cases} W = \iint_S \left(\vec{f} \cdot \vec{u}\right) dS \quad , \; dS = r d\theta dx \\ \left(\vec{f} \cdot \vec{u}\right) dS = \left(P_i r_i - P_o r_o\right) U_z d\theta dx \end{cases} \tag{15}$$

P_i and P_o are the horizontal pressures in the internal and external surfaces. Variation of the strain energy can be expressed as follows

$$\begin{cases} \delta U = R \int_0^{2\pi} \int_0^L \int_{-h/2}^{h/2} \delta U^* \left(1+\frac{z}{R}\right) dz dx d\theta \\ \Rightarrow \frac{\delta U}{2\pi} = R \int_0^L \int_{-h/2}^{h/2} (\sigma_x \delta\varepsilon_x + \sigma_\theta \delta\varepsilon_\theta + \sigma_z \delta\varepsilon_z + \tau_{xz}\delta\gamma_{xz}) \left(1+\frac{z}{R}\right) dz dx \end{cases} \tag{16}$$

And the variation of the external work is

$$\begin{cases} \delta W = \int_0^{2\pi} \int_0^L \left[P_i r_i - P_o r_o\right] \delta U_z dx d\theta \\ \Rightarrow \frac{\delta W}{2\pi} = \int_0^L \left[P_i \left(R - \frac{h}{2}\right) - P_o \left(R + \frac{h}{2}\right)\right] \delta U_z dx \end{cases} \tag{17}$$

By substituting Eqs. (4), (6) and (8) into Eqs. (16)-(17) and by using Eq. (13), and carrying out the integration by parts, the equilibrium equations are obtained in the form of

$$\begin{cases} R\dfrac{dN_x}{dx}=0 \\ R\dfrac{dM_x}{dx}-RQ_x=0 \\ R\dfrac{dQ_x}{dx}-N_\theta=-P_i\left(R-\dfrac{h}{2}\right)+P_o\left(R+\dfrac{h}{2}\right) \\ R\dfrac{dM_{xz}}{dx}-M_\theta-RN_z=P_i\dfrac{h}{2}\left(R-\dfrac{h}{2}\right)+P_o\dfrac{h}{2}\left(R+\dfrac{h}{2}\right) \end{cases} \tag{18}$$

And the boundary conditions at the two ends of cylinder are

$$R\left[N_x\delta u+M_x\delta\varphi+Q_x\delta w+M_{xz}\delta\psi\right]_0^L=0 \tag{19}$$

Eq. (18) expresses the main governing equations based on the FSDT for the cylindrical shells under internal and/or external pressure. Eq. (19) is the boundary conditions which should be satisfied at two end of the cylinder.

In fact, Eq. (18) is the set of differential equations. In order to solve the set of Eq. (18), forces and moments should be written by the usage of Eqs. (9) to (12) in the terms of displacement field. Finally a set of linear non-homogenous differential equations with constant coefficients would be resulted as follows

$$[A]\frac{d^2}{dx^2}\{y\}+[B]\frac{d}{dx}\{y\}+[C]\{y\}=\{F\} \tag{20}$$

Where $\{y\}$ is the unknown vector including the components of displacement field, $[A]_{4\times4}$, $[B]_{4\times4}$ and $[C]_{4\times4}$ are the coefficients matrices and $\{F\}$is the force vector which can be expressed as the non-homogeneity of the set of differential equations. The coefficient matrices $[A]$ and $[C]$ are symmetric while $[B]$ is anti-symmetric. The coefficient matrices have been defined in the appendix.

Matrix $[C]$ is irreversible and its reverse is needed in the next calculations. In order to make $[C]^{-1}$, the first equation in the set of Eq. (18) is integrated.

$$RN_x=C_0 \tag{21}$$

In Eq. (18), it is apparent that u does not exist, but du/dx does. In Eq. (4), du/dx is needed to calculate displacements, therefore by assuming $du/dx=v$ as a new parameter which could be indicated in the following terms

$$u=\int v\,dx+C_7 \tag{22}$$

By the mentioned changes, the unknown vector $\{y\}$ in the set of differential Eq. (18) can be rewritten as follows

$$\{y\}=\{v \quad \varphi \quad w \quad \psi\}^T \tag{23}$$

Also non-homogeneity of the differential Eq. (18) can be derived as follows

$$\{F\}=\frac{1}{\lambda E_i^*}\begin{Bmatrix} C_0 \\ 0 \\ -P_i\left(R-\frac{h}{2}\right)+P_o\left(R+\frac{h}{2}\right) \\ P_i\frac{h}{2}\left(R-\frac{h}{2}\right)+P_o\frac{h}{2}\left(R+\frac{h}{2}\right) \end{Bmatrix} \tag{24}$$

3. Analytical solution

The Eq. (18) has the general solution $\{y\}_g$ and the particular solution $\{y\}_p$, as follows

$$\{y\}=\{y\}_g+\{y\}_p \tag{25}$$

For the general solution, $\{y\}_g=\{V\}e^{mx}$ is substituted in homogeneous Eq. (20).

$$e^{mx}\left(m^2[A_1]+m[A_2]+[A_3]\right)\{V\}=\{0\} \tag{26}$$

Considering that e^{mx} is not equal to zero, the following determinant which is equal to zero would be resulted.

$$\left|m^2[A_1]+m[A_2]+[A_3]\right|=0 \tag{27}$$

The determinant above is a six-order polynomial which is a function of m, the roots of which are the eigenvalues m_i consist of 3 pairs of conjugated root. Substituting the calculated eigenvalues in Eq. (26), the corresponding eigenvectors $\{V\}_i$ are obtained. Therefore, the general solution has been resulted.

$$\{y\}_g=\sum_{i=1}^{6}C_i\{V\}_i e^{m_i x} \tag{28}$$

Given that $\{F\}$ is comprised of constant parameters, for the non-homogenous part of solution of Eq. (20), the particular solution can be expressed as follows.

$$[C]\{y\}_p=\{F\}\Rightarrow\{y\}_p=[C]^{-1}\{F\} \tag{29}$$

Finally, the total solution is a summation of the general and the particular solution.

$$\{y\}=\sum_{i=1}^{6}C_i\{V\}_i e^{m_i x}+[A_3]^{-1}\{F\} \tag{30}$$

Constants $C_1,\ldots,C_6$ in the general solution and two constants C_0, C_7 which have been resulted by the mathematical calculus will be obtained by applying eight boundary conditions.

Given that the two ends of the cylinder are clamped-clamped, then

$$\begin{Bmatrix} u \\ \varphi \\ w \\ \psi \end{Bmatrix}_{x=0} = \begin{Bmatrix} u \\ \varphi \\ w \\ \psi \end{Bmatrix}_{x=L} = \begin{Bmatrix} 0 \\ 0 \\ 0 \\ 0 \end{Bmatrix} \tag{31}$$

4. Results and discussion

As a case study, we consider a thick cylinder whose elasticity modulus varies in radial direction and has the following characteristics: r_i=40 mm, h=20 mm and L=0.8 m. The modulus of elasticity at the internal radius and Poisson's ratio have values of E_i=200 GPa and v=0.3, respectively. The applied internal pressure is P_i=80 MPa. The analytical solution is carried out by writing the program in MAPLE 13.

In order to show the abilities of the presented analytical solution for analyzing a FG cylinder, a numerical solution has been investigated. The ANSYS 13 package was used in the static analysis of thick hollow cylinder with constant thickness. The PLANE82 element in axisymmetric mode, which is an element with eight nodes and two translational degrees of freedom in the axial and radial directions per each node, was used for discretization. In order to consider the radial continuous varying of elastic modulus along the thickness of cylindrical shell with an exponential function, the thickness of cylinder has been divided to some homogeneous layers. Each layer's properties have been defined as an exponential function of the distance of layer's middle from internal layer. Finally the cylindrical shell consists of some coherent homogeneous layers which properties at the contact location of the layers are the average of left and right limit of two layers' boundaries. Dividing the thickness of the cylinder into 40 layers causes the results of numerical modeling to converge to the results of analytical solution. Considering more than 40 layers have no considerable effect on the results of FEM. Internal pressures are applied to the nodes of inner layers. Clamped boundary conditions have been exerted by preventing the nodes around two ends of the cylinder from movement. The numerical and analytical results have been investigated for clamped-clamped boundary conditions.

The distribution of the normalized radial displacement resulted from the numerical and analytical solution at middle of a cylinder is depicted in Fig. 3. It is seen that for negative values of n, the displacements of FGM cylinders are higher than of a homogeneous cylinder. For positive values of n, the situation is reverse, i.e., the displacement is lower. The variation in the displacement of heterogeneous material is similar to that of homogenous material. It is obviously observed in Fig. 3 that the radial displacements have its maximum values in internal surface ($z=-h/2$). Figs. 4-5 show the distribution of the normalized radial and axial displacement along the axial in the middle surface of the cylinder for different inhomogeneity constants. The radial displacement at points away from the boundaries depends on radius and length. It is observed that middle of the cylinder has no axial displacement. For n<0 axial displacements of the cylinder are more than homogeneous material while for n>0 is smaller.

Distribution of dimensionless circumferential stress in different layers are shown in Figs. 6-7 for $n=\pm1$. The circumferential stress at all points depends on radius and length. The circumferential stress at layers close to the external surface at points near boundary is negative, and at other layers positive. The greatest circumferential stress occurs in the internal surface ($z=-h/2$). Distribution

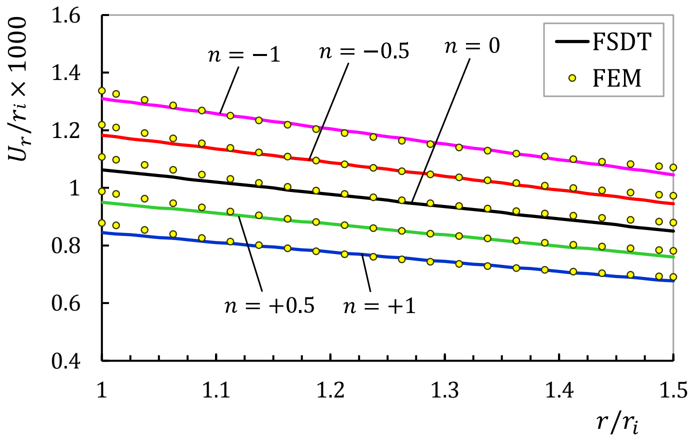

Fig. 3 Radial displacement distribution at middle of the cylinder

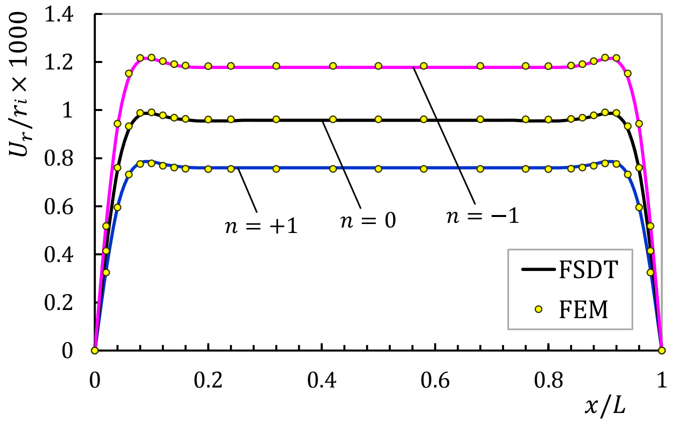

Fig. 4 Radial displacement distribution in the middle surface

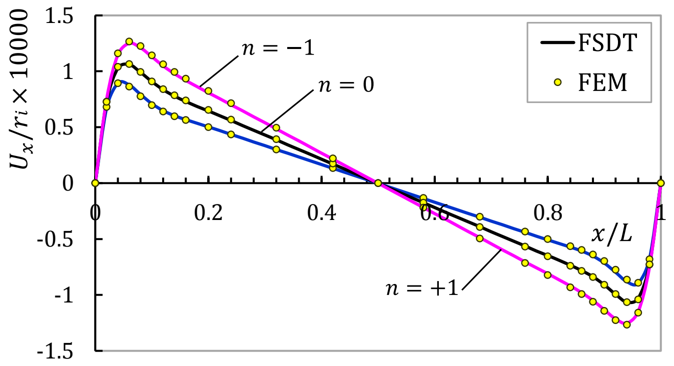

Fig. 5 Axial displacement distribution in middle surface

of dimensionless axial stress in different layers are shown in Figs. 8-9 for n=±1. At points away from the boundaries, axial stress unlike the circumferential stress does not show significant differences in different layers, while at points near the boundaries, the reverse holds true for both

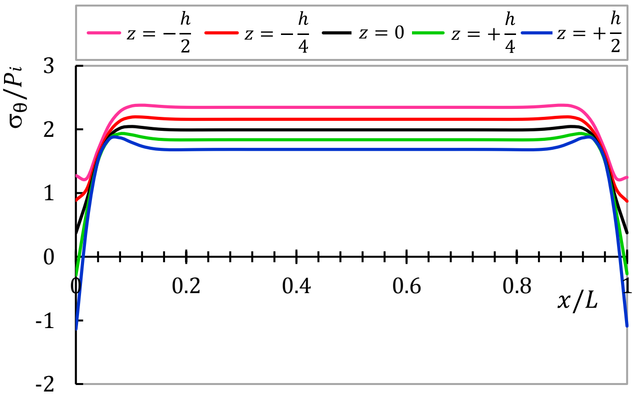

Fig. 6 Circumferential stress distribution in different layers for *n*=+1

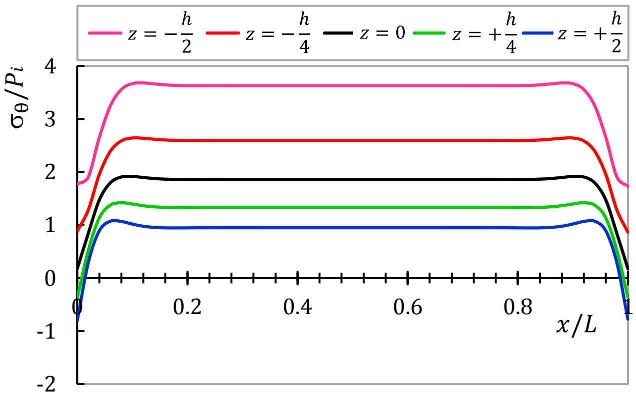

Fig. 7 Circumferential stress distribution in different layers for *n*=−1

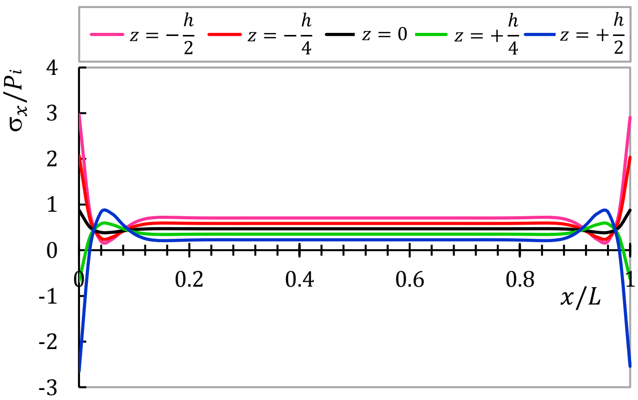

Fig. 8 Axial stress distribution in different layers for *n*=+1

of stresses. Figs. 10-11 show the distribution of shear stress along the longitude of cylinder for $n=\pm 1$ in different layers. It is obviously observed that there are shear stresses near two ends of the cylinder. The shear stress at points away from the boundaries at different layers is the same and trivial. However, at points near the boundaries, the stress is significant.

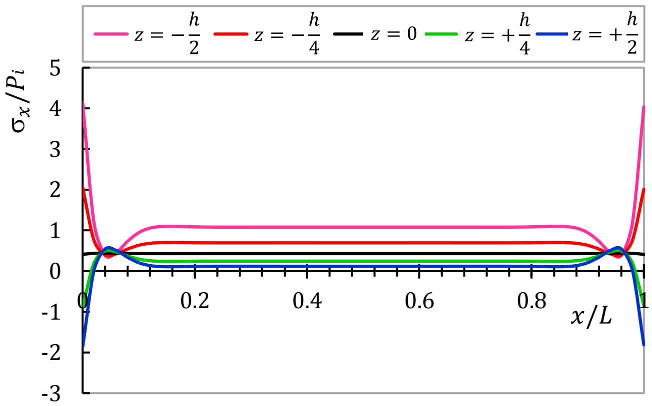

Fig. 9 Axial stress distribution in different layers for *n*=−1

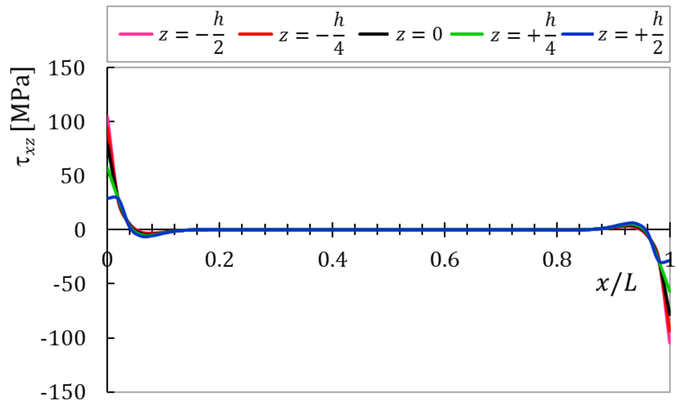

Fig. 10 Shear stress distribution in different layers for *n*=+1

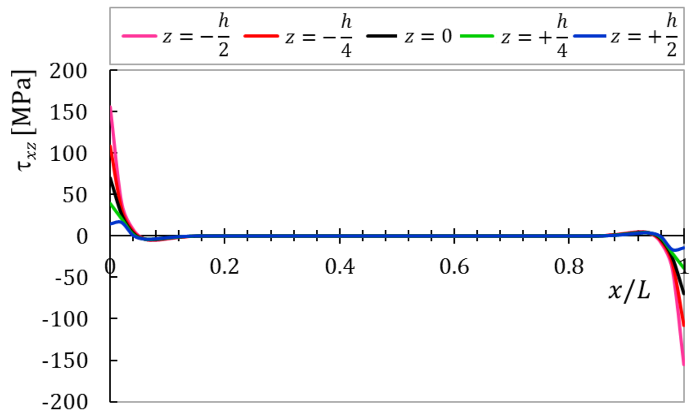

Fig. 11 Shear stress distribution in different layers for *n*=−1

Tables 1-2 presents the results of the different solutions for the middle of the heterogeneous cylinder (*x*=*L*/2) and middle surface (*z*=0). The results suggest that in points further away from the boundary it is possible to make use of classical theory (PET).

Table 1 Numerical results of radial displacement for x=L/2 and z=0

		n=−1	n=−0.5	n=0	n=+0.5	n=+1
u_r, mm	FSDT	0.04710	0.04260	0.03826	0.03420	0.03040
	FEM	0.04677	0.04252	0.03843	0.03418	0.03022

Table 2 Numerical results of stresses for x=L/2 and z=0

		n=−1	n=−0.5	n=0	n=+0.5	n=+1
σ_x, MPa	FSDT	34.31	35.34	36.23	36.96	37.50
	FEM	35.90	35.94	36.21	35.51	35.51
σ_θ, MPa	FSDT	148.8	152.6	155.6	157.9	159.4
	FEM	151.0	154.0	156.1	157.5	158.4

5. Conclusions

In this research, the heterogeneous hollow cylinders with radially exponentially varying elastic modulus, have been solved by FSDT and FEM, and have been compared with homogenous cylinders. In the present study, the advantages as well as the disadvantages of the classical theory (PET) for hollow thick-walled cylindrical shells were indicated. Regarding the problems which could not be solved through PET, the solution based on the FSDT is suggested. At the boundary areas of a thick- walled cylinder with clamped-clamped ends, having constant thickness and uniform pressure, given that displacements and stresses are dependent on radius and length, use cannot be made of PET, and FSDT must be used. The shear stress in boundary areas cannot be ignored, but in areas further away from the boundaries, it can be ignored. Therefore, the PET can be used, provided that the shear strain is zero. The maximum displacements and stresses in all the areas of the cylinder occur on the internal surface. The analytical solutions and the solutions carried out through the FEM show good agreement.

References

Eipakchi, H.R., Rahimi, G.H. and Khadem, S.E. (2003), “Closed form solution for displacements of thick cylinders with varying thickness subjected to nonuniform internal pressure”, *Struct. Eng. Mech.*, **16**(6), 731-748.

Eipakchi, H.R., Khadem, S.E. and Rahimi, G.H. (2008), “Axisymmetric stress analysis of a thick conical shell with varying thickness under nonuniform internal pressure”, *J. Eng. Mech.*, **134**, 601-610.

Fukui, Y. and Yamanaka, N. (1992), “Elastic analysis for thick-walled tubes of functionally graded materials subjected to internal pressure”, *JSME, Ser. I*, **35**(4), 891-900.

Ghannad, M. and Zamani Nejad, M. (2010), “Elastic analysis of pressurized thick hollow cylindrical shells with clamped-clamped ends”, *Mechanika*, **5**(85), 11-18.

Ghannad, M. and Zamani Nejad, M. (2012), “Complete elastic solution of pressurized thick cylindrical shells made of heterogeneous functionally graded materials”, *Mechanika*, **18**(6), 640-649.

Greenspon, J.E. (1960), “Vibration of a thick-walled cylindrical shell, comparison of the exact theory with approximate theories”, *J. Acoust. Soc. Am.*, **32**(5), 571-578.

Hongjun, X., Zhifei, S. and Taotao, Z. (2006), “Elastic analyses of heterogeneous hollow cylinders”, *J. Mech., Res. Commun.*, **33**(5), 681-691.

Mirsky, I. and Hermann, G. (1958), “Axially motions of thick cylindrical shells”, *J. Appl. Mech. Tran.*

ASME, **25**, 97-102.

Simkins, T.E. (1994), "Amplifications of flexural waves in gun tubes", *J. Sound Vib.*, **172**(2), 145-154.

Tutuncu, N. (2007), "Stresses in thick-walled FGM cylinders with exponentially-varying properties", *J. Eng. Struct.*, **29**, 2032-2035.

Vlachoutsis, S. (1992), "Shear correction factors for plates and shells", *Int. J. Numer. Math. Eng.*, **33**, 1537-1552.

Zamaninejad, M., Rahimi, G.H. and Ghannad, M. (2009), "Set of field equations for thick shell of revolution made of functionally graded materials in curvilinear coordinate system", *Mechanika*, **3**(77), 18-26.

Zhifei, S., Taotao, Z. and Hongjun, X. (2007), "Exact solutions of heterogeneous elastic hollow cylinders", *Compos. Struct.*, **79**(1), 140-147.

Appendix

$$A_{11} = (1-\nu)\int_{-h/2}^{+h/2} e^{\frac{nz}{r_i}} (R+z)\,dz \tag{32}$$

$$A_{12} = A_{21} = (1-\nu)\int_{-h/2}^{+h/2} e^{\frac{nz}{r_i}} (R+z)\,z\,dz \tag{33}$$

$$A_{22} = (1-\nu)\int_{-h/2}^{+h/2} e^{\frac{nz}{r_i}} (R+z)\,z^2\,dz \tag{34}$$

$$A_{33} = \mu\int_{-h/2}^{+h/2} e^{\frac{nz}{r_i}} (R+z)\,dz \tag{35}$$

$$A_{34} = A_{43} = \mu\int_{-h/2}^{+h/2} e^{\frac{nz}{r_i}} (R+z)\,z\,dz \tag{36}$$

$$A_{44} = \mu\int_{-h/2}^{+h/2} e^{\frac{nz}{r_i}} (R+z)\,z^2\,dz \tag{37}$$

$$A_{13} = A_{31} = A_{14} = A_{41} = A_{23} = A_{32} = A_{24} = A_{42} = 0 \tag{38}$$

$$B_{13} = -B_{31} = \nu\int_{-h/2}^{+h/2} e^{\frac{nz}{r_i}}\,dz \tag{39}$$

$$B_{14} = -B_{41} = \nu\int_{-h/2}^{+h/2} e^{\frac{nz}{r_i}} (R+2z)\,dz \tag{40}$$

$$B_{23} = -B_{32} = \int_{-h/2}^{+h/2} e^{\frac{nz}{r_i}} \left[(\upsilon-\mu)z-\mu R\right]dz \tag{41}$$

$$B_{24} = -B_{42} = \int_{-h/2}^{+h/2} e^{\frac{nz}{r_i}} \left[(\nu-\mu)R+(2\nu-\mu)z\right]z\,dz \tag{42}$$

$$B_{11} = B_{12} = B_{21} = B_{22} = B_{33} = B_{34} = B_{43} = B_{44} = 0 \tag{43}$$

$$C_{22} = -\mu \int_{-h/2}^{+h/2} e^{\frac{nz}{r_i}} \left(R + z\right) dz \tag{44}$$

$$C_{33} = -\left(1-\nu\right) \int_{-h/2}^{+h/2} e^{\frac{nz}{r_i}} \frac{dz}{R + z} \tag{45}$$

$$C_{34} = C_{43} = -\int_{-h/2}^{+h/2} e^{\frac{nz}{r_i}} \left[\nu + \frac{(1-\nu)z}{R+z}\right] dz \tag{46}$$

$$C_{44} = -\int_{-h/2}^{+h/2} e^{\frac{nz}{r_i}} \left[2\nu z + \frac{(1-\upsilon)z^2}{R+z} + (1-\nu)(R+z)\right] dz \tag{47}$$

$$C_{11} = C_{12} = C_{21} = C_{13} = C_{31} = C_{14} = C_{41} = C_{23} = C_{32} = C_{24} = C_{42} = 0 \tag{48}$$

Where the parameter μ is as follows

$$\mu = \frac{5}{12}\left(1 - 2\nu\right) \tag{49}$$